# Deuterium and Carbon-13 NMR Study of a Banana Mesogen: Molecular Structure and Order

**ARTICLE** *in* THE JOURNAL OF PHYSICAL CHEMISTRY B · JUNE 2004

Impact Factor: 3.3 · DOI: 10.1021/jp0498264

# Deuterium and Carbon-13 NMR Study of a Banana Mesogen: Molecular Structure and Order

**Ronald Y. Dong,*,†,‡ K. Fodor-Csorba,§ J. Xu,† V. Domenici,|| G. Prampolini,|| and C. A. Veracini||**

*Department of Physics and Astronomy, University of Manitoba, Winnipeg, MB, Canada R3T 2N2, Department of Physics and Astronomy, Brandon University, Brandon, MB, Canada R7A 6A9, Research Institute of Solid State Physics and Optics, Budapest, Konkoly Thege u. 29-33, Hungary, and Departimento di Chemica e Chimica Industriale, Universita di Pisa, Via Risorgimento 35, 56126, Italy*

*Received: January 13, 2004; In Final Form: April 2, 2004*

The orientational order and the molecular structure of the banana mesogen 4-chloro-1,3-phenylene bis{4,4′-(11-undecenyloxy)benzoyloxy}benzoate have been studied in its nematic phase by means of $^2$H and $^{13}$C NMR. A detailed discussion of orientational order parameters for either the entire molecular core or the selectively deuterated fragments, and geometrical features concerning the rigid core of the molecule is given. In particular, the angles $\theta_i$ between the para axis of the aromatic ring and the long molecular axis for each lateral wing are estimated. Quantum chemical calculations on the rigid core made by the central five aromatic rings, employing the B3LYP density functional method, support the molecular structure derived from the NMR results. This study shows how important is the comparison between $^2$H and $^{13}$C NMR to better understand the real structure of banana-shaped compounds in their mesophases and further sheds light on the open question about chirality or achirality of banana molecules.

## Introduction

One of the most surprising results in the study of soft matter in the last 10 years was the prediction that fluid biaxial smectic phases formed from compounds *without* asymmetric carbons could, by symmetry, have a spontaneous polarization in the layer plane.[1−3] Such molecules are now known as banana mesogens because of their bent molecular shape.[4] Several classes of banana molecules have been synthesized in the last 4−5 years;[5] physical properties of these materials could span from ferroelectricity−antiferroelectricity for electrooptical applications, to second harmonic generation in nonlinear optics, to highly efficient electrets for broad-band telecommunications. Therefore, though there is enormous scientific interest in these materials, there seems to be a huge potential for high-tech applications as well. In ferroelectric smectic phases mirror symmetry is broken because of the presence of one or more chiral centers; in the case of banana molecules the symmetry is broken spontaneously because the molecular shape is not rodlike but bow- or banana-shaped. Spontaneous optical resolution is long known in crystals, but this spontaneous breaking of mirror symmetry in "liquids" has very recently gained large interest also outside the LC community. When found in soft matter, it can be expected to have nontrivial effects particularly in biology and biochemistry because of the importance of chiral recognition and self-assembling in supramolecular structures and functions.

It has often been stated that such materials, consisting of achiral molecules, may form chiral smectic layers. This statement, however, could be not completely correct; in fact, very poor knowledge is available at the moment concerning the detailed molecular structure of banana molecules. These molecules are generally formed by a central benzene group with two meta substituents (the lateral wings), connected to the central ring with a para-substituted benzoyl ester group (see Figure 1). If the two lateral substituents, the wings, are twisted in opposite directions, then the molecule can assume a propeller shape. This situation is called *atropoisomerism* in organic chemistry. Recently, simple molecular mechanics calculations have shown that an asymmetry in orientation of the two lateral wings with respect to the central ring is possible.[6] To confirm this first and new theoretical result, either more accurate quantum mechanical calculations or experimental data, in particular coming from NMR, could be useful.

Few papers concerning $^{13}$C NMR investigations on banana-shaped molecules have been published in the past few years,[7−10] showing the possibility of accessing geometrical information, such as the bending angle, but at the same time these studies have revealed that the analyses of $^{13}$C NMR spectra need the knowledge of the orientation and components of the chemical shift anisotropy (CSA) tensor of each carbon in the molecule. An incorrect evaluation of these quantities could introduce nonnegligible errors in either the local order parameter $S_{zz}$ or the molecular geometry. In fact, only recently, $^1$H and $^{19}$F NMR studies[11,12] have been introduced to support $^{13}$C NMR. On the other hand $^2$H NMR spectroscopy gives precise information although restricted to the deuterated positions, and the synthesis of samples labeled in different sites is quite expensive. A meaningful improvement in knowledge of molecular structure of banana-shaped mesogens could come from the comparative analysis of $^2$H and $^{13}$C NMR spectra and this is the main motivation of this work.

† University of Manitoba.
‡ Brandon University.
§ Research Institute of Solid State Physics and Optics.
|| Universita di Pisa.

10.1021/jp0498264 CCC: $27.50 
Published on Web 05/18/2004

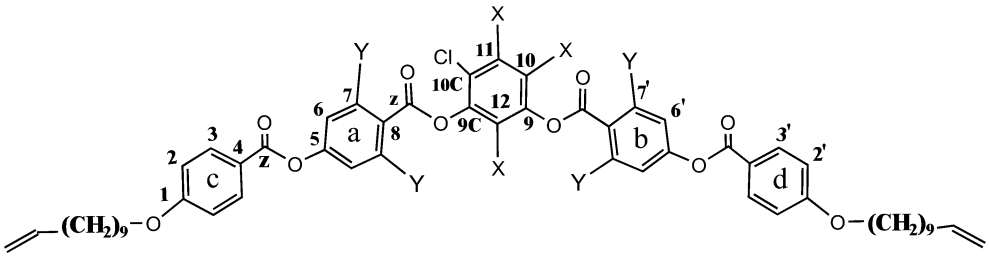


**Figure 1.** Molecular structure of the nonlabeled banana-shaped mesogen ClPbis11BB (X = $^1$H, Y = $^1$H) and the two labeled samples ClPbis11BB-$d_3$ (X = $^2$H, Y = $^1$H) and ClPbis11BB-$d_4$ (X = $^1$H, Y = $^2$H).

## Experimental Section

**Samples.** The banana-shaped mesogen 4-chloro-1,3-phenylene bis{4,4′-(11-undecenyloxy)benzoyloxy}benzoate (C1Pbis11BB) and the two selectively deuterated samples, either on the central ring (ClPbis11BB-$d_3$) or on the first two lateral phenyl rings (ClPbis11BB-$d_4$) (see Figure 1), have been investigated by means of $^{13}$C and $^2$H NMR, respectively. The synthesis and characterization of the nonlabeled sample and the two labeled ones are reported respectively on refs 6 and 13. The phase transition temperatures of the labeled sample C1Pbis11BB, detected by optical microscopy and differential scanning calorimetry,[6] in the cooling cycle are given here:

Iso 82 °C (SmC 49 °C) N 38 °C Cr and
Iso 72 °C (SmC 40 °C) N 27 °C Cr

It must be noticed that the transition temperatures observed from the NMR spectra for the three samples are slightly different from those reported in the literature, probably due to impurities, isotopic substitutions, and/or different experimental conditions.

**$^2$H NMR.** The $^2$H NMR experiments were carried out on a 9.40 T Varian InfinityPlus400, working at 61.38 MHz, and on a 7.05 T Varian VXR300 spectrometer, working at 46.04 MHz, for the samples ClPbis11BB-$d_3$ and ClPbis11BB-$d_4$, respectively. The samples were macroscopically aligned within the magnet by slow cooling from the isotropic phase; the $^2$H spectra were recorded every 2 deg allowing 10 min for thermal equilibration, either with or without $^1$H continuous-wave decoupling. The 90° pulse was 2.8 $\mu$s and 16.0 $\mu$s for the two spectrometers, respectively. The temperature was stable within 0.2 deg, for both instrumentations.

**$^{13}$C NMR.** The $^{13}$C NMR experiments were performed on a Bruker Avance 400 spectrometer operating at 100.6 MHz. The 1D and 2D $^{13}$C NMR spectra of the nonlabeled C1Pbis11BB in $CDCl_3$ were performed in the high resolution (HR) mode using a BBI probe. The 1D $^{13}$C spectrum was obtained by using a single carbon pulse and the FID collected with the Waltz-16 proton decoupling sequence. The $^{13}$C peak assignments were aided by the well-known DEPT (distortionless enhancement by polarization transfer) and 2D $^{13}$C−$^1$H correlation (XHCORR) experiments.[14] The 1D $^{13}$C NMR experiments of the static neat sample were done with a two-channel HX solid probe. The isotropic phase spectrum was collected as in the HR mode except the Waltz-16 decoupling power was higher. The $^{13}$C spectra in the nematic phase were collected using standard cross polarization (CP, 2 ms) after the 90° proton irradiation. Proton decoupling during the $^{13}$C signal acquisition was done by the SPINAL-64 pulse sequence[15] with a minimal decoupling field of ca. 10 kHz. To avoid sample heating, the recycle delay between each FID acquisition was 6 s. Each spectrum was obtained after signal averaging 512 or fewer scans. The temperature calibration was made for a given air flow using the known phase transition temperatures of a liquid crystal. The

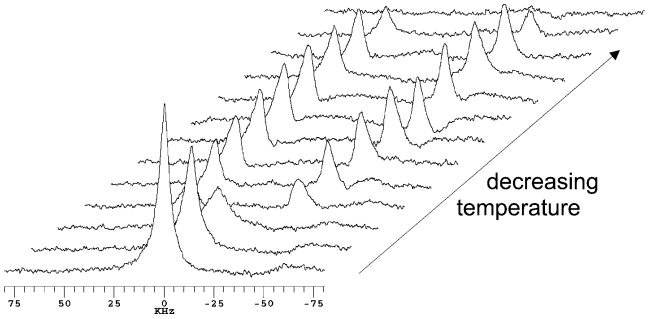


**Figure 2.** $^2$H NMR spectra of the mesogen ClPbis11BB-$d_3$ from $T$ = 84 °C to $T$ = 60 °C every 2 deg.

$^{13}$C peak assignments in the aligned sample were based on experiments using the pulse sequence of simultaneous phase inversion (PI) and CP (i.e., CPPI),[16] and previous $^{13}$C peak assignments in similar compounds.[9,17,18] In the CPPI spectrum, one should see negative $CH_2$, null CH, and positive nonprotonated C signals. The $^1$H 90° pulse width was 3.9 $\mu$s and the temperature gradient across the sample was estimated to be within 0.3 deg.

## Results and Discussion

**$^2$H NMR.** The $^1$H-decoupled spectra obtained on cooling the two samples ClPbis11BB-$d_3$ and ClPbis11BB-$d_4$ from isotropic phase (bottom spectra) to the crystalline phase (top spectra) are shown in Figures 2 and 3, respectively. The clearing point can be observed from the drastic change of the $^2$H spectrum passing from the isotropic to the nematic phase. In the case of ClPbis11BB-$d_3$ the temperature transition is between 80 and 78 °C and the nematic phase ranges from 78 °C to 62 °C, after which the sample crystallizes. For the sample deuterated on the lateral wings, ClPbis11BB-$d_4$, the transitions isotropic−nematic and nematic-crystal occur at about 72 and 52 °C, respectively.

In both cases, the spectrum of the isotropic phase consists of a single peak, due to the presence of aromatic deuterons, which do not have meaningful differences in the chemical shift value. As can be seen in either Figure 2 or 3, the isotropic peak shows a very unusual line-width broadening in a large range of temperature above the clearing point (for instance, from 2500 to 15 000 Hz in a range of about 20 deg for the ClPbis11BB-$d_3$), which is due mainly to dynamic processes, as has been suggested in a recent study,[19] where a detailed analysis, also supported by $T_2$ relaxation time measurements, has been reported.

The $^2$H spectrum in the nematic phase is generally characterized by a quadrupolar doublet for each type of deuterium, which distinguishes among other types of deuterons either by the quadrupolar constant $\nu_q$ (for instance aliphatic versus aromatic deuterons), by geometrical factors (angle between the C−D bond and the local principal axis), or by order parameters, which can be different for each local fragment. In the case of ClPbis11BB-

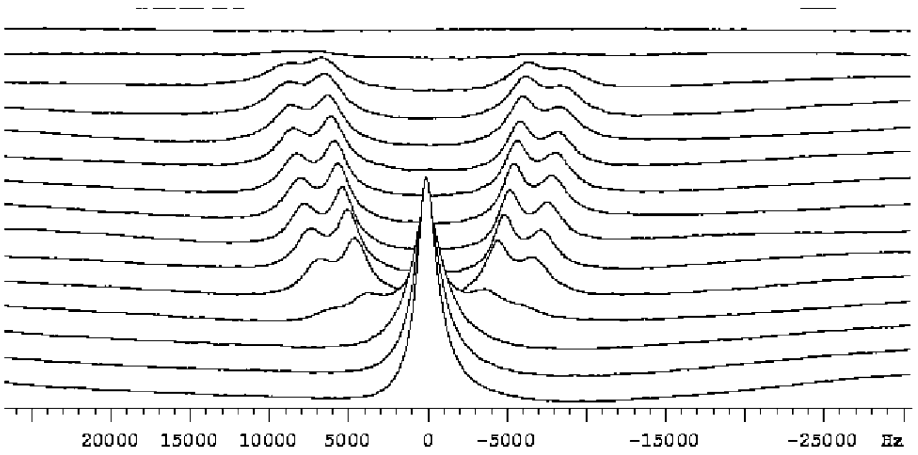


**Figure 3.** $^2$H NMR spectra of the mesogen ClPbis11BB-$d_4$ from $T = 78$ °C (bottom spectrum) to $T = 50$ °C (top spectrum) every 2 deg.

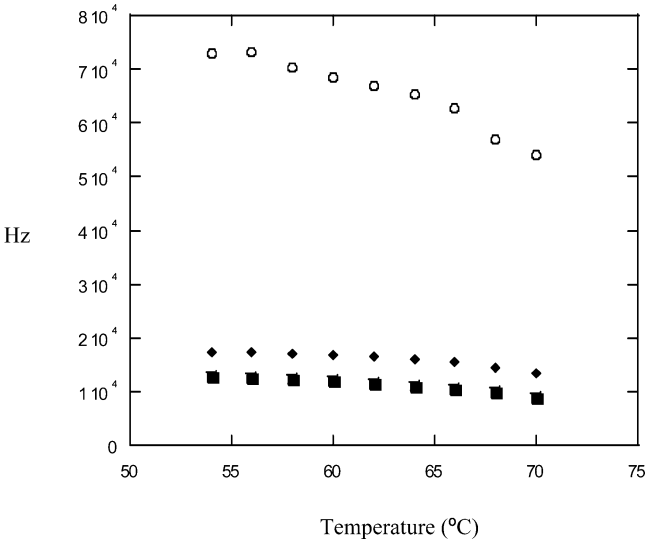


**Figure 4.** Quadrupolar splittings (Hz) as a function of temperature (°C). Empty circles represent aromatic deuterons of the central ring (ClPbis11BB-$d_3$), and full squares and full rhomb symbols represent the deuterium types (**a** and **b**, respectively) belonging to the first lateral phenyl rings (ClPbis11BB-$d_4$). Note that the temperature has been shifted for the ClPbis11BB-$d_3$ to match the clearing points for the two mesogens.

$d_3$ a single very large doublet can be observed with a line width of about 7500 Hz; thus the quadrupolar splitting, which is measured as the distance in hertz from the top of the two peaks, is affected by an estimated error of about ±500 Hz, larger than in common rodlike liquid crystals.[20−22] The $^2$H NMR spectrum of ClPbis11BB-$d_4$ in the nematic phase consists of two quadrupolar doublets partially superimposed, which nevertheless allows one to measure the two quadrupolar splittings, corresponding to the aromatic deuterons belonging to the two different wings. In Figure 4 quadrupolar splittings of the different deuterium nuclei in the nematic phase of the two samples are reported as a function of the temperature, after having shifted the clearing point of ClPbis11BB-$d_3$ to match that of ClPbis11BB-$d_4$.

Because $^1$H-decoupled and $^1$H-coupled spectra do not show any particular difference, $^1$H−$^2$H dipolar couplings are not measurable and the analysis to obtain information on the orientational order can be performed by considering the quadrupolar splittings only. It has been assumed that the two types of deuterium nuclei of the sample ClPbis11BB-$d_3$, "1" and "2", which are clearly shown in Figure 5, contribute to the same quadrupolar splitting but with opposite sign. To prove the

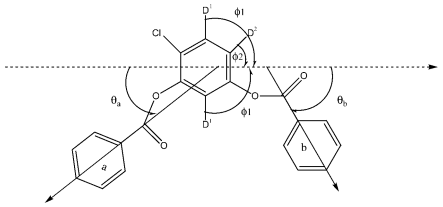


**Figure 5.** Scheme of the central core structure. The arrows indicate the direction of the long molecular axis (dashed one) and that of the local para axis in the two lateral phenyl rings "**a**" and "**b**" (solid ones). Angles $\theta_a$, $\theta_b$, $\phi_1$, and $\phi_2$ shown in the figure are calculated from the fitting analysis, and the superscript on the deuterons indicates the type (1 or 2) of deuterium.

validity of such an assumption, the order parameter $S_{zz}(T)$ and the biaxiality $\Delta_{biax}$ of the central phenyl ring, as well as the angles $\phi^i$ between the C−D bonds and the long molecular axis, indicated by a dashed arrow in Figure 5, have been determined by fitting the experimental quadrupolar splitting to the following equation:[23]

$$\Delta\nu^i_q[T] = \frac{3}{2}q_{\mathbf{aa}}\left\{S_{zz}[T]\left(\cos^2\phi^i - \frac{1}{2}\sin^2\phi^i - \frac{\eta}{6}\cos^2\phi^i + \frac{\eta}{6} + \frac{\eta}{3}\sin^2\phi^i\right) + \Delta_{biax}\left(\frac{1}{2}\sin^2\phi^i + \frac{\eta}{6}\cos^2\phi^i + \frac{\eta}{6}\right)\right\} \quad (1)$$

where the deuterium quadrupolar coupling constant $q_{\mathbf{aa}} = 185$ kHz, the asymmetric parameter $\eta = 0.04$, and $i$ indicates the type of deuteron ("1" or "2"). The biaxiality and the angles $\phi^i$ have been assumed constant throughout the temperature range investigated. Using a nonlinear fitting procedure, we obtain 12 best-fitting parameters (nine values for $S_{zz}$, one for each temperature, one value of biaxiality, and two values of angles) by analyzing nine experimental quadrupolar splittings for both "1" and "2" nuclei. The best-fitting parameters concerning the geometry of the central ring are $\phi^1 = 89.6 \pm 0.5°$ and $\phi^2 = 35.6 \pm 0.5°$, which confirm the proposed interpretation. The local order parameter $S_{zz}$ of the central phenyl ring ranges from 0.407 to 0.549 by decreasing temperature, as reported in Figure 6. To determine the value of biaxiality, it must be noted that the experimental error on the measured quadrupolar splittings is quite critical, although the $\Delta_{biax}$ found from the fitting is substantially very low (from 0.002 to practically 0 value).

The order parameters $S_{zz}^{\mathbf{a}}$ and $S_{zz}^{\mathbf{b}}$, relative to the para axis of the two phenyl rings **a** and **b**, have been calculated from the quadrupolar splittings by using eq 1, assuming $\Delta_{biax} = 0$ for both fragments[24] and the angles $\phi^i$ between the C−D bonds and the para axes equal to 60°;[19,21] the trends of such order

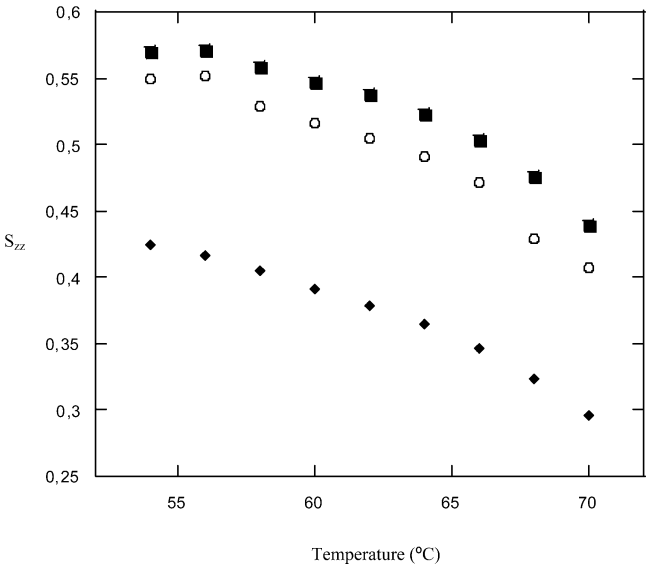


**Figure 6.** Local order parameters $S_{zz}^i$ as a function of temperature (°C). Empty circles, full squares, and full rhomb symbols represent the order parameters relative to the central ring (ClPbis11BB-$d_3$) and the para axes of the phenyl rings "**a**" and "**b**" (ClPbis11BB-$d_4$), respectively.

parameters as a function of temperature are shown in Figure 6. On the basis of these results, we can also estimate the angles $\theta_i$, indicated in Figure 5, between the para axes of the two phenyl fragments, **a** and **b**, and the long molecular axis, by the following equation:

$$\theta_i = \arccos\left[\sqrt{\frac{2(S_{zz}^{\text{more ordered}})/(S_{zz}^{\text{less ordered}}) + 1}{3}}\right] \quad (2)$$

where the calculated values of order parameters are used. The average values of the angle $\theta_\mathbf{a}$ and $\theta_\mathbf{b}$ so found are 11.8° and 23.9°, respectively.

**Quantum Chemical Calculations.** Quantum chemical calculations have been carried out employing the B3LYP[25] density functional method, with the 6-31G double-$\zeta$ basis set, by the use of the Gaussian 98 package.[26] The main goal of these calculations is to understand which conformations of the lateral wings with respect to the central core of ClPbis11BB are favored and how these can influence the orientation of the para axes with respect to the long molecular axis and, hence, the overall shape of the molecule. On the assumption that one can neglect, in first approximation, the effect of the aliphatic side chains on the torsional conformations of the central core of the mesogen, all calculations were performed on the 4-chloro-1,3-phenylene bis{4,4′-(methoxy)benzoyloxy}benzoate molecule (see Figure 7). With this aim, a geometry optimization was performed first without imposing any symmetry restriction. The optimized geometry is shown in Figure 7. The molecule results in a planar conformation with the torsional angles $\phi_\mathbf{a}$ and $\phi_\mathbf{b}$, defined as the dihedrals formed by atoms 1−2−3−4 and 1′−2′−3′−4′, measuring 180° and 0°, respectively. Moreover, these different values reflect in different values of $\theta_\mathbf{a}$ and $\theta_\mathbf{b}$, (12° and 49°) defined, as done in $^2$H NMR, as the angles between the para axis $S_\mathbf{a}$ and $S_\mathbf{b}$ and the long molecular axis $S_{zz}$ (see Figure 5). Due to the extended $\pi$ conjugation and to the absence of steric hindrance, the outer rings remain coplanar to the inner ones.

Clearly, other three planar conformations, which conserve extended conjugation, are possible, namely those with $\phi_\mathbf{a}$ ($\phi_\mathbf{b}$) measuring 180° (180°), 0° (180°), and 0° (0°), respectively. Recent DFT calculations,[27] performed on the 1,3-phenylene bis-

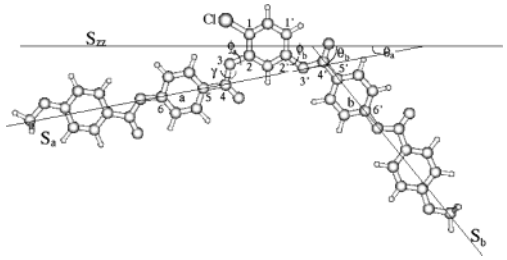


**Figure 7.** Central core of the banana-shaped mesogen used in quantum chemical calculations. $S_{zz}$, $S_\mathbf{a}$, and $S_\mathbf{b}$ define the long molecular axis and the para axis of ring **a** and **b**, respectively. $\theta_\mathbf{a}$ and $\theta_\mathbf{b}$ are the angles of the $S_\mathbf{a}$ and $S_\mathbf{b}$ axis with $S_{zz}$. The dihedrals $\phi_\mathbf{a}$ and $\phi_\mathbf{b}$ are those formed by atoms 1, 2, 3, 4 and 1′, 2′, 3′, 4′, respectively, and the dihedral $\gamma$ is defined by atoms 2, 3, 4, 5.

{4,4′-(methoxy)benzoyloxy}benzoate molecule (i.e., the molecule treated in the present study with the chloride atom substituted by a hydrogen), have shown that the all-trans conformation $\phi_\mathbf{a} = \phi_\mathbf{b} = 180°$ is energetically unfavorable, due to the repulsive nature of the interaction between the dipoles of the inner carboxylic groups of the two wings. This feature should not be altered by the presence, in this study, of the chloride atom on the central ring. The other planar conformations can be obtained by imposing $\phi_\mathbf{a} = 0°$. To investigate their stability, a further calculation has been performed, with the restriction of $\phi_\mathbf{a} = 0°$. In this case the optimized geometry shows quite different features with respect of the former: although the **b** ring is still coplanar to the central one (with $\phi_\mathbf{b} = 180°$), the "wing" containing the **a** ring rotates out of the central ring plane of almost 45°. Because the $\phi_\mathbf{a}$ dihedral was constrained at 0°, this conformation is achieved by varying the $\gamma$ torsional angle (formed by atoms 2−3−4−5; see Figure 7) from 180° (equilibrium value) to 133°.

The driving force of this rotation is probably due to the electrostatic repulsion between the chloride atom of the central ring and the carboxylic oxygen bonded to atom 4. Indeed, the energy barrier of 11.5 kcal/mol, found with respect of the minimum geometry ($\phi_\mathbf{a} = 180°$; $\phi_\mathbf{b} = 0°$), suggests that it is very unlikely that at room temperature the molecule, even in bulk phase, can assume such conformation.

Focusing on the minimum energy conformation, the value obtained for $\theta_\mathbf{a}$ is concordant with the average value (11.8°) proposed by $^2$H NMR measurements, suggesting that the **a** "wing" is coplanar with the central ring and the oxygen atom is in trans position with respect of the chlorine atom. On the contrary, the $\phi_\mathbf{b}$ value of 0°, found in the optimized geometry implies an angle $\theta_\mathbf{b}$ of 49°, which is about 2 times that found by $^2$H (23.9°) measurements. The main question that arises is whether the presence of neighboring molecules in the bulk phase can yield intermolecular forces such as to induce the **b** wing to adopt a $\phi_\mathbf{b}$ angle other than 0°.

Also, it is interesting to see which dihedral angle the **b** wing should assume to yield a $\theta_\mathbf{b}$ angle consistent with that reported by NMR. With this goal, several geometry optimizations were performed, with no symmetry restriction except for the torsional angle $\phi_\mathbf{b}$. The curve showing the dependence of $\theta_\mathbf{b}$ on the $\phi_\mathbf{b}$ values is reported in Figure 8. It can be noted that when the considered dihedral angle has a value of 135°, the angle between $S_\mathbf{b}$ and $S_{zz}$ is of 24.8°, in close agreement with the value from $^2$H NMR measurements. Because the energy barrier of this conformation with respect to the planar minimum geometry is about 1.2 kcal/mol, the population of this conformation in the bulk phase cannot be excluded. We now turn to $^{13}$C NMR of this banana mesogen to seek further confirmation of the above $^2$H NMR and quantum chemical findings.

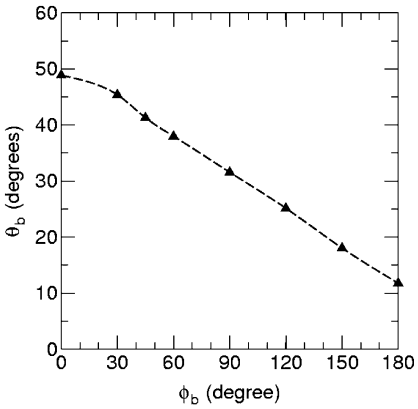


**Figure 8.** Dependence of angle $\theta_b$ (see Figure 7) on $\phi_b$ as from DFT optimizations.

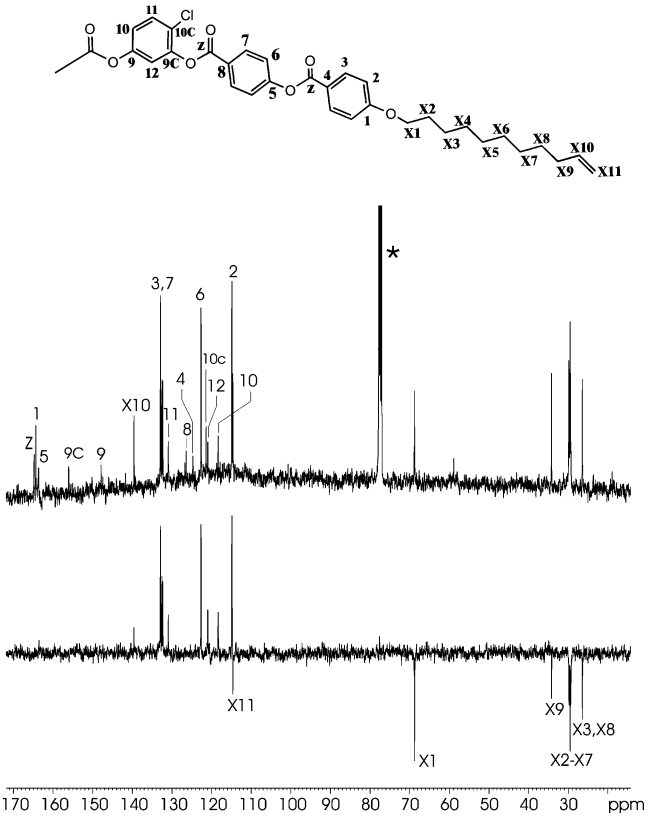


**Figure 9.** High-resolution C-13 spectra of C1Pbis11BB/$CDCl_3$ solution at room temperature. The asterisk denotes an impurity peak due to slight ethanol.

**$^{13}$C NMR.** Figure 9 shows the HR $^{13}$C NMR spectra of ClPbis11BB/$CDCl_3$ together with the $^{13}$C peak assignments. The bottom trace is a DEPT spectrum in which $CH_2$ signals are negative, CH signals positive, and null signals for all nonprotonated carbons. Isotropic chemical shifts of protons were assigned first in a HR proton spectrum (not shown). Figure 10 shows the HXCORR spectrum with the peak assignments according to the $^1$H and $^{13}$C isotropic chemical shifts. Figure 11 shows some typical $^{13}$C spectra obtained in a static ClPbis11BB sample at several temperatures. The aligned sample in the magnetic field was obtained by cooling from the isotropic (I) phase to the nematic (N) phase. During the phase transition from I to N, $^{13}$C chemical shifts $\delta$ of the aromatic carbons increase markedly but those of the aliphatic carbons decrease slightly (i.e., upfield shifts). Note that carbon peaks shown in the isotropic phase (bottom trace) are significantly broadened in comparison with those shown in Figure 9. The uncertainty

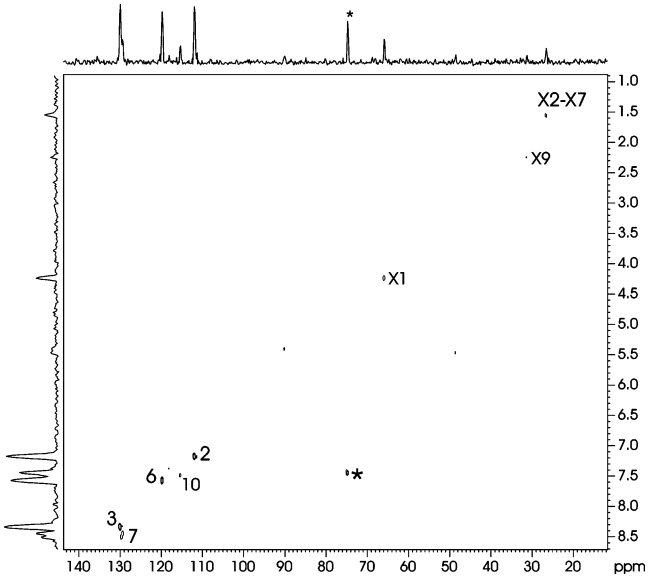


**Figure 10.** 2D HXCORR spectrum of C1Pbis11BB/$CDCl_3$ solution at room temperature. The asterisk denotes an impurity peak.

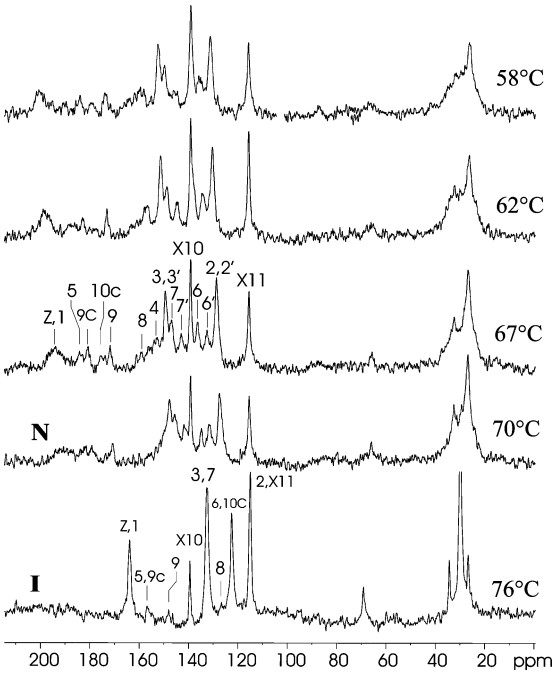


**Figure 11.** $^{13}$C NMR spectra of the field-aligned C1Pbis11BB sample at 100.6 MHz.

in the measured $\delta_{iso}^{(j)}$ is ca. ±1 ppm for both the protonated and nonprotonated carbons. The assignment of $^{13}$C peaks, in the N phase shown in Figure 11, was aided by the CPPI experiment whose spectrum at 69 °C is shown in Figure 12. Here the nonprotonated carbons show positive peaks and $CH_2$ signals are negative, whereas the CH signals are nearly null. The temperature dependence of $\delta^{(j)}$ shown in Figure 11 for the aromatic carbons and the X10 and X11 carbons are plotted in Figure 13. For aromatic carbons, the least shielded element is in the ring plane radially pointing out from the ring, and the most shielded element is perpendicular to the ring plane. As the nematic director is aligned along the external field, a downfield shift of the aromatic lines is expected (see Figure 13). It is noted that $\delta$(T) of the X10 and X11 carbons are almost temperature insensitive, and our peak assignments for carbons 9, 9c, and 10c of the central ring are tentative. It is also clear from Figure 11 that the aliphatic carbon peaks are closely

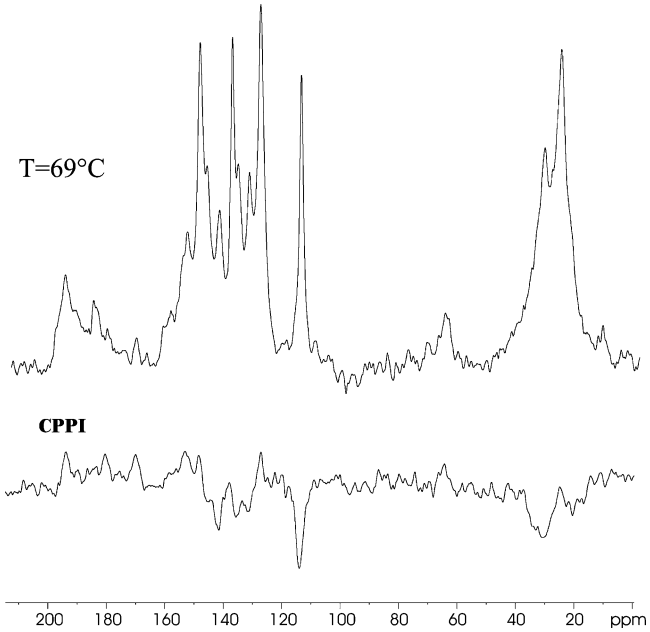


**Figure 12.** 1D $^{13}$C NMR CP and CPPI spectra of the C1Pbis11BB sample at the same temperature.

overlapped except for X10 and X11, and the present $^{13}$C study, therefore, focuses on the aromatic carbons from the side rings.

The chemical shift $\sigma$ in a liquid crystalline phase is related to the isotropic chemical shift $\delta_{iso}$, the components of the chemical shift tensor $\delta_{ij}$, and order parameter $S_{ij}$ according to[28]

$$\delta = \delta_{iso} + \frac{2}{3}S_{zz}\{\delta_{zz} - (\delta_{xx} + \delta_{yy})/2\} + \frac{1}{3}(\delta_{xx} - \delta_{yy}) \times (S_{xx} - S_{yy}) + \frac{2}{3}(S_{yz}\delta_{yz} + S_{xz}\delta_{xz} + S_{xy}\delta_{xy}) \quad (3)$$

As a first approximation, the banana molecule is assumed to rotate rapidly about its long molecular axis (see Figure 5). Because of rapid rotations, $S_{xy}$, $S_{yz}$ and $S_{xz}$ vanish, and $S_{xx} - S_{yy}$ is usually small in uniaxial mesophases. With these restrictions,

$$\delta = \delta_{iso} + \frac{2}{3}S(\delta_{||} - \delta_{\perp}) \quad (4)$$

where $\delta_{||}$ is the chemical shift component along the direction of the long molecular $z$ axis, $\delta_{\perp} = (\delta_{xx} + \delta_{yy})/2$ is the average chemical shift component along a short molecular axis, and $S$ ($=S_{zz}$) is the nematic order parameter associated with the long molecular axis. In the simple case of a rapid rotation about the long axis, $\delta_{||}$ and $\delta_{\perp}$ are given by

$$\delta_{||} = (\cos^2\alpha\cos^2\beta)\delta_{11} + (\sin^2\alpha\sin^2\beta)\delta_{22} + (\cos^2\beta)\delta_{33}$$

$$\delta_{\perp} = \frac{1}{2}(1 - \cos^2\alpha\sin^2\beta)\delta_{11} + \frac{1}{2}(1 - \sin^2\alpha\sin^2\beta)\delta_{22} + \frac{1}{2}(\sin^2\beta)\delta_{33} \quad (5)$$

where $\alpha$ and $\beta$ are the polar angles for $\delta_{ij}$ in the molecular frame. Because of the uncertainty in the assignments of carbon peaks from the central ring, we have concentrated on fitting the chemical shift data of $C_1$ to $C_8$ from the two side rings (**a**, **c** or **b**, **d** in Figure 1) on each wing of the banana molecule. The $^{13}$C data can be used to determine the angles $\theta_i$ formed by the para axes of all rings **a**−**d** with respect to the long molecular $z$ axis. As seen in Figure 11, only one line is observed for each

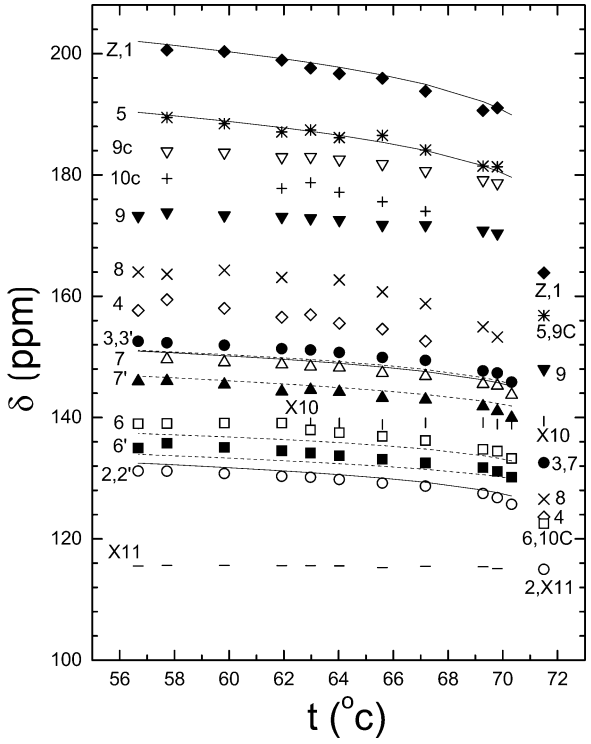


**Figure 13.** Plot of $^{13}$C chemical shifts for various carbons (site labels same as in Figure 1) as a function of temperature. $T_c = 71$ °C.

pair of aromatic carbons in the ortho position from these side rings. This implies that the phenyl rings (**a**−**d**) must perform at least 180° ring flips. For aromatic carbons on these rings, there is an additional coordinate transformation from their para axes ($x_p$, $y_p$, $z_p$) to the long molecular $z$ axis resulting in the following $\delta$ expression:

$$\delta^{(j)} = \delta_{iso}^{(j)} + \frac{2}{3}SP_2(\cos\theta_i)\left[\left(-\frac{1}{2} + \frac{3}{2}\cos^2\alpha^{(j)}\sin^2\beta^{(j)}\right)\delta_{11}^{(j)} + \left(-\frac{1}{2} + \frac{3}{2}\sin^2\alpha^{(j)}\sin^2\beta^{(j)}\right)\delta_{22}{}^{(j)} + P_2(\cos\beta^{(j)})\delta_{33}^{(j)}\right] \quad (6)$$

where $\alpha^{(j)}$ and $\beta^{(j)}$ are the polar angles for the $\delta_{ij}^{(j)}$ of the $j$th carbon in the ($x_p$, $y_p$, $z_p$) frame. The $x_pz_p$ plane is defined by the plane of the central ring. The principal axis system (1, 2, 3) for the chemical shift tensor is chosen by assuming that the 3 axis is along the C−H bond or C−C bond and the 1 axis is normal to the $x_pz_p$ plane. This assumption is necessary as the chemical shift tensor for various carbons in this banana molecule is unavailable. When the side ring is coplanar to the central ring, the 1 axis is, therefore, also normal to this ring plane, making $\alpha = 90°$. In an attempt to estimate the order parameter and orientation of the different fragments in the banana core from eq 6, we make use of the fact that the general features of chemical shift (shielding) tensors have been determined for aromatic carbons of model compounds from single-crystal studies.[29,30] In addition, chemical shift tensors of aromatic carbons obtained from other compounds such as chiral liquid crystals, to a first approximation, are also used in the present study.[17,31] This approach has been used in the past to estimate the order parameter from liquid crystalline materials.[18,32] The principal elements of $\delta$ tensors for the model compounds used in this study are listed in Table 1, together with calculated $\delta_{iso}$ and the corresponding experimental values found in the isotropic phase of neat sample. Within the experimental uncertainties, the calculated $\delta_{iso}$ for the listed carbons are close to the observed isotropic chemical shifts. For the para carbons 4 and 8, we fail

**TABLE 1: Chemical Shift Tensors for Various Carbon Sites**[a]

| sites | 1[b] | 2[c] | 3,7[d] | 5[e] | 6[e] |
|---|---|---|---|---|---|
| $\delta_{11}$ | 67.8 | 8.7 | 15 | 74 | 23 |
| $\delta_{22}$ | 169.3 | 135.5 | 153 | 162 | 104 |
| $\delta_{33}$ | 244 | 192.6 | 226 | 230 | 211 |
| $\delta_{iso}$(calc) | 160.4 | 112.3 | 131.3 | 155.3 | 119 |
| $\delta_{iso}$(expt) | 163.9 | 115.4 | 132.8 | 157 | 122.5 |

[a] Note that $\delta_{ii} = \sigma_{ref} - \sigma_{ii}$ is used to give the last 3 columns, where $\sigma_{ref}$ is the chemical shielding of a reference compound. [b] Reference 17. [c] Reference 31. [d] Reference 29. [e] Reference 30.

to find a set of $\delta_{ij}$ that can reproduce the observed isotropic chemical shifts. Thus, the following calculations utilize the observed chemical shifts from carbons 1, 2, 3, 5, 6, and 7 only. As seen in Figure 11, the $^{13}$C signals of rings **c** and **d** appear to be identical indicating that their para axes make more or less the same $\theta$ angle. When all rings in the wings are coplanar with the central ring, then $\alpha = 90°$ in the above equation. In the first instance, this $\alpha$ value is used. For **a** and **b** rings, the ortho and meta carbons clearly show doubling (i.e., get four $^{13}$C peaks for 6, 6′, 7, and 7′ instead of two) in $^{13}$C signals, whereas this has not been identified for the para carbons because of the spectral resolution and S/N. The observation is possible if $\theta_{\mathbf{a}}$ is different from $\theta_{\mathbf{b}}$ as suggested above. For the protonated carbon, the $\beta$ angle between the CH bonds (along the 3 axis) and the para axis of each side ring has the nominal value of 60°. For the para carbons, $\beta = 0$. As seen in eq 6, the change in the chemical shift $\Delta\delta^{(j)}$ can only give the product $S$ and $P_2(\cos\theta_i)$ and our data cannot untangle the order parameter $S$ and the angle $\theta_i$ unambiguously. We have therefore chosen to fix one of the $\theta_i$, i.e., $\theta_{\mathbf{a}}$ equal to 11.8° at all temperatures, as suggested in the deuteron results. Now by fitting the observed chemical shifts at each temperature, one can calculate $S$ for each carbon site and its associated unknown angle $\theta_i$ if applicable. We found that (a) $\theta_{\mathbf{b}}$, $\theta_{\mathbf{c}}$, and $\theta_{\mathbf{d}}$ are almost temperature insensitive, (b) the chemical shifts of sites 1 and 1′ (2, 2′ or 3, 3′) are almost identical, whereas those of 5 and 5′ are dissimilar. Hence in the following analysis, we have taken the average value of the chemical shifts for carbons 5 and 5′ to fit the observed chemical shift from these sites. We have carried out a global target analysis of all the $\Delta\delta$'s for $C_1$ to $C_7$ and $C_1$′ and $C_7$′ (4, 4′ excluded) given in Figure 11 to obtain $S$, $\theta_{\mathbf{b}}$, $\theta_{\mathbf{c}}$, and $\theta_{\mathbf{d}}$ by minimizing the sum square error using the routine AMOEBA.[33] To do this, we have adopted the temperature dependence of $S$ using the Haller equation[34]

$$S(T) = S_0(1 - T/T^*)^f$$

where $S_0$ and $f$ are empirical constants and $T^*$ is the temperature slightly above $T_c$ (=344 K) at which $S$ becomes 0. We have set $T^* = 345$ K, and the weak temperature behavior of $\theta_i$ ($i = \mathbf{b}$, **c**, **d**) is given by $\theta_i = \theta'_i + \eta_i(T - T_c)$. In the global analysis, $S_0$, $f$, $\theta'_i$, and $\eta_i$ are the variables to give the best fits to the chemical shifts at 11 temperatures. We found that the calculated chemical shifts are in close agreement with the observed values in the nematic phase although systematic deviations do exist, in particular carbons 3 and 6. The $S$ values are somewhat lower than those obtained by deuterium NMR (e.g., at $T_C$ $S = 0.355$) average $\theta_{\mathbf{b}} = 26.4°$, and average $\theta_{\mathbf{c}}$ = average $\theta_{\mathbf{d}} = 16.4°$. Next, we consider the possibility of twisting the ring plane of **b** ring out of the $x_p z_p$ plane by an angle $\phi$ such that for this ring, $\alpha = 90° - \phi$ in eq 6. We found that the fits are improved when $\phi = 14°$ (the sum-square-error decreases by about 16%). We have, therefore, chosen to present the results of the global analysis

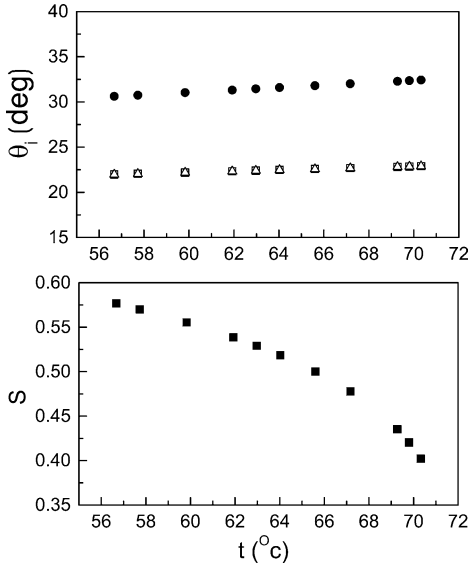


**Figure 14.** Plots of the order parameter $S$ and angles $\theta_i$ for ring **b** (solid circles), ring **c** (open triangles), and ring **d** (open squares) as a function of temperature in the nematic phase of C1Pbis11BB.

with this twist angle for ring **b**. The calculated $\delta$'s are shown as solid curves in Figure 13 with $S_0 = 0.96$ and $f = 0.16$. As seen in this figure, the experimental chemical shifts in the nematic phase for the studied sites are reproduced satisfactorily. The average values of $\theta_{\mathbf{b}}$, $\theta_{\mathbf{c}}$, and $\theta_{\mathbf{d}}$ are equal to 31.6°, 21.5°, and 21.5°, respectively. We note that with a nonzero twist angle for ring **b**, the fitted $\theta_i$ values are now larger by about 5°. Figure 14 summarizes the order parameter $S$ and $\theta_i$ as a function of temperature. The $S$ values are now same as $S_{zz}$ determined by $^2$H NMR within experimental errors, which is encouraging despite the numerous approximations used in the present analysis. The out of the central ring plane for the lateral wing containing the ring **b** is possible with only a minimal energy, as suggested by the quantum mechanical calculations. When the average $\theta_{\mathbf{b}}$ values from the deuteron and carbon-13 studies are compared, they differ by about 8°. The carbon-13 $\theta_{\mathbf{b}}$ value is higher by 33%, which can be due to experimental errors and/or uncertainties in the chemical shift tensors adopted for the calculations. The bending angle $\Psi$ subtended by the two side wings of the banana molecule is determined as 136.6° from the angles $\theta_{\mathbf{b}}$ and $\theta_{\mathbf{a}}$. This angle is almost the same (137°) if measuring from the two outer rings $\theta_{\mathbf{d}}$ and $\theta_{\mathbf{c}}$. It is, nevertheless, larger than the value of 127.6° reported for another banana molecule.[35] It should be noted that the above deuterium NMR data cannot tell whether the **b** ring is coplanar or not with the central ring. In summary, the present $^{13}$C results collaborate the findings of the deuterium results from three deuterated rings in ClPbis11BB.

## Conclusions

The present study has demonstrated the utility of $^2$H and $^{13}$C as a powerful way to gain information on the molecular structure and ordering of banana molecules. With the help of deuterium results, one can have confidence on the choice of chemical shift tensors for various carbon sites, and their spectral assignments. The banana mesogen studied here does not seem to give a planar molecular core and the bending angle (ca. 137°) is larger due to a monosubstituted chlorine in the central ring.

Quantum chemical calculations are useful for examining the molecular conformation, even though care must be taken in the choice of the method and the basis set. In fact, a more detailed

study on the inclusion of polarization in the employed basis set is now in progress in our laboratory.[27] However, some preliminary conclusions can still be drawn. The torsional potential curve appears to be very flat, and many conformations, differing in $\phi_{\mathbf{a}}$ and $\phi_{\mathbf{b}}$ values, can be populated in the condesed phases. In particular, the relatively small barrier ($\approx$1 kcal/mol) does not rule out the possibility for the mesogen core to assume those chiral conformations ($\phi_{\mathbf{a}} \neq \phi_{\mathbf{b}}$) suggested by the $^2$H NMR and quantum chemical calculations. Moreover, two other interesting features can be underlined. First, the external phenyl rings tend to be coplanar to the inner ones, so that the two wings can be treated in first approximation as two biaxial rigid rotors. Second, because the presence of the Cl atom forces the **a** wing to assume values of $\phi_{\mathbf{a}}$ near to 180°, the overall molecular shape results in a more "rodlike" structure, making the angle subtended by the two wings larger than the non-chlorinated homologue. It may be interesting to notice that the latter molecule does not yield any nematic phase, giving raise, on the contrary, to B2 liquid crystals. Finally, the angles $\theta_{\mathbf{b}}$ determined by the $^{13}$C and $^2$H studies differ by about 8°, and such difference may well be due to the lack of knowledge of $^{13}$C chemical shift tensors for the studied mesogen.

**Acknowledgment.** We are grateful to Italian MIUR for partial financial support, and to Prof. Ivo Cacelli for the many useful discussions. K.F.C. is grateful to the Hungarian Research Grant OTKA for the T030401 and T32667 suport. R.Y.D. acknowledges the financial support from the Natural Sciences and Engineering Council of Canada, Canada Foundation for Innovation, and Brandon University. The technical support of N. Finlay is also acknowledged.

## References and Notes

(1) Prost, J.; Barois, P. *J. Chem. Phys*. **1983**, *80*, 65.
(2) Petschek, R. G.; Wiefling, K. M. *Phys. Rev. L ett.* **1987**, *59*, 343.
(3) Tournilhac, F.; Blinov, L. M.; Simon, J.; Yablonski, S. V. *Nature* **1992**, *359*, 621.
(4) Niori, T.; Sekine, F.; Watanabe, J.; Furukawa, T.; Takezoe, H. *J. Mater. Chem.* **1996**, *6*, 1231.
(5) Pelzl, G.; Diele, S.; Weissflog, W. *Adv. Mater*. **1999**, *11*, 707.
(6) Fodor-Csorba, K.; Vajda, A.; Galli, G.; Jakli, A.; Demus, D.; Holly, S.; Gacs-Baitz, E. *Macromol. Chem. Phys.* **2000**, *203*, 1556.
(7) Weissflog, W.; Lischka, Ch.; Diele, S.; Pelzl, G.; Wirth, I.; Grande, S.; Kresse, H.; Schmalfuss, H.; Hartung, H.; Stettler, A. *Mol. Cryst. Liq. Cryst.* **1998**, *333*, 203.
(8) Diele, S.; Grande, S.; Kruth, H.; Lischka, Ch.; Pelzl, G.; Weissflog, W.; Wirth, I. *Ferroelectrics* **1998**, *212*, 169.
(9) Pelzl, G.; Grande, S.; Jakli, A.; Lischka, Ch.; Kresse, H.; Schmalfuss, H.; Wirth, I.; Weissflog, W. *Liq. Cryst.* **1999**, *26*, 401.
(10) Dehne, H.; Potter, M.; Sokolowski, S.; Weissflog, W.; Diele, S.; Pelzl, G.;, Wirth, I.; Kresse, H.; Schmalfuss, H.; Grande, S. *Liq. Cryst.* **2001**, *28*, 1269.
(11) Eremin, A.; Wirth, I.; Diele, S.; Pelzl, G.; Schmalfuss, H.; Kresse, H.; Nadasi, H.; Fodor-Csorba, K.; Gacs-Baitz, E.; Weissflog, W. *Liq. Cryst.* **2002**, *29*, 775.
(12) Nadasi, H.; Weissflog, W.; Eremin, A.; Pelzl, G.; Diele, S.; Das, B.; Grande, S. *J. Mater. Chem.* **2002**, *12*, 1316.
(13) Domenici, V.; Fodor-Csorba, K.; Holly, S.; Gacs-Baitz, E.; Veracini, C. A. To be submitted.
(14) Bax, A.; Morris, G. A. *J. Magn. Reson*. **1981**, *42*, 501.
(15) Fung, B. M.; Khitrin, A. K.; Ermolaev, K. *J. Magn. Reson*. **2000**, *142*, 97.
(16) Wu, X.; Zilm, K. W. *J. Magn. Reson. A* **1993**, *102*, 205.
(17) Nakai, T.; Fujimori, H.; Kuwahara, D.; Miyajima, S. *J. Phys. Chem. B* **1999**, *103*, 417.
(18) Yoshizawa, A.; Kikuzaki, H.; Fukumasa, M. *Liq. Cryst*. **1995**, *18*, 351.
(19) Blinc, R.; Domenici, V.; Lebar, A.; Geppi, M.; Veracini, C. A.; Zalar, B.; To be submitted.
(20) Catalano, D.; Cavazza, M.; Chiezzi, L.; Geppi, M.; Veracini, C. A. *Liq. Cryst.* **2000**, *27*, 621.
(21) Catalano, D.; Chiezzi, L.; Domenici, V.; Geppi, M.; Veracini, C. A.; Dong, R. Y.; Fodor-Csorba, K. *Macromol. Chem. Phys.* **2002**, *203*, 1594.
(22) Catalano, D.; Chiezzi, L.; Domenici, V.; Geppi, M.; Veracini, C. A. *J. Phys. Chem. B* **2003**, *107*, 10104.
(23) Veracini, C. A. NMR spectra in Liquid Crystals the Partially Averaged Spin Hamiltonian. In *Nuclear Magnetic Resonance of Liquid Crystals*; Emsley, J. W.. Ed.; Reidel: Dordrecht, The Netherlands, 1985: Vol. 141, Chapter 5, p 99.
(24) Calucci, L.; Catalano, D.; Fodor-Csorba,K.; Forte, C.; Veracini, C. A. *Mol. Cryst. Liq. Cryst.* **1999**, *331*, 1869.
(25) Becke, A. D. J. *Chem. Phys.* **1993**, *98*, 5648.
(26) Frisch, M. J.; et al. *Gaussian 98*, revision A1; Gaussian Inc.: Pittsburgh, PA, 1998.
(27) Cacelli, I.; Prampolini, G. Work in progress.
(28) Wemmer, D. E.; Pines, A. *J. Am. Chem. Soc*. **1981**, *103*, 34.
(29) Wemmer, D. E.; Pines, A.; Whitehurst, D. D. *Philos. Trans. R. Soc. A* **1981**, *300*, 15.
(30) Maricq, M. M.; Waugh, J. S. *J. Chem. Phys*. **1979**, *70*, 3300.
(31) Zheng, G.; Hu, J.; Zhang, X.; Shen, L.; Ye, C.; Webb, G. A. *J. Mol. Struct. (THEOCHEM)* **1998**, *428*, 283.
(32) Oulyadi, H.; Laupretre, F.; Monnerie, L.; Mauzac, M.; Richard, H.; Gasparoux, H. *Marcromolecules* **1990**, *23*, 1965.
(33) (33) Press, W. H.; Flannery, B. P.; Teukolsky, S. A.; Vetterling, W. T. *Numerical Recipes*; Cambridge University: Cambridge, England, 1986.
(34) Haller, I. V. *Prog. Solid State Chem*. **1975**, *10*, 103.
(35) Kinoshita, Y.; Park, B.; Takezoe, H.; Nion, T.; Watanabe, J. *Langmuir* **1998**, *14*, 6256.